



Contents lists available at ScienceDirect

Journal of Biomechanics

journal homepage: www.elsevier.com/locate/jbiomech
www.JBiomech.com

An in vitro model of impaction during hip arthroplasty

Ruben Doyle^a, Oliver Boughton^{a,b}, Daniel Plant^d, George Desoutter^c, Justin P. Cobb^b, Jonathan R.T. Jeffers^{a,*}^a Department of Mechanical Engineering, Imperial College London, London, SW7 2AZ, UK^b Sackler Centre for Musculoskeletal Research, Department of Surgery & Cancer, Imperial College London, London, W6 8RP, UK^c De Soutter Medical Limited, Aston Clinton, Buckinghamshire, HP22 5WF, UK^d Rheon Labs Ltd., 11S Hewlett House, Havelock Terrace, London, SW8 4AS, UK

ARTICLE INFO

Article history:

Accepted 23 October 2018

Keywords:

Hip arthroplasty
Impaction
In-vitro testing
Boundary conditions
Compliance

ABSTRACT

Impaction is required to properly seat press-fit implants and ensure initial implant stability and long term bone ingrowth, however excessive impaction or press-fit presents a high fracture risk in the acetabulum and femur. Current in-vitro impaction testing methods do not replicate the compliance of the soft tissues surrounding the hip, a factor that may be important in fracture and force prediction. This study presents the measurement of compliance of the soft tissues supporting the hip during impaction in operative conditions, and replicates these in vitro. Hip replacements were carried out on 4 full body cadavers while impact force traces and acetabular/femoral displacement were measured. Compliance was then simulated computationally using a Voigt model. These data were subsequently used to inform the design of a representative in-vitro drop rig. Effective masses of 19.7 kg and 12.7 kg, spring stiffnesses of 8.0 kN/m and 4.1 kN/m and dashpot coefficients of 595 N s/m and 322 N s/m were calculated for the acetabular and femoral soft tissues respectively. A good agreement between cadaveric and in-vitro peak displacement and rise time during impact is found. Such an in-vitro setup is of use during laboratory testing, simulation or even surgical training.

© 2018 Elsevier Ltd. All rights reserved.

1. Introduction

The use of cementless implants for Total Hip Arthroplasty (THA) in the UK surpassed that of cemented in 2009, and the majority of THA implants used in Europe, Scandinavia, Australia and the US are also cementless (American Joint Replacement Registry, 2016; Graves et al., 2014; NJR Editorial Board, 2014; Pedersen and Fenstad, 2016). Cementless implants require precise implantation through impact strikes, usually delivered with a mallet, and an appropriate interference fit with the prepared bone. The impaction and interference fit need to be sufficient to provide primary fixation, but not so much that they cause deformation of the components or generate high strains in the bone. Issues due to improper impaction are widely reported. Acetabular cup deformation of over 0.5 mm has been recorded under worst case conditions (Squire et al., 2006) which is clinically important as deformations can lead to excessive wear (Daniel et al., 2012) or improper compo-

nent assembly (Langdown et al., 2007; Rehmer et al., 2012). High impact forces can also lead to fracture of both the acetabular and femoral bone (Benazzo et al., 2015; Hartford and Knowles, 2018; Lindberg-larsen et al., 2017; Masri et al., 2004; Sharkey et al., 1999; Thien et al., 2014; Thillemann et al., 2008).

Therefore it is important to understand the impaction forces and fixation mechanisms that occur when a femoral or acetabular component is press-fit in the bone. A wide range of values exist for impaction force in THA surgery – between 1.5 kN and 27 kN have been measured for implant seating in the acetabulum (Fritsche et al., 2008; Kroeber et al., 2002; West and Fryman, 2008) or between 5.8 kN and 22 kN for the femoral stem (Maharaj and Jamison, 1993; West and Fryman, 2008). Further to these data, femoral bone has been reported to fracture at between 0.5 kN and 4 kN stem impaction (Cummins et al., 2011; Flannery et al., 2010).

The wide range of values reported may be at least partly explained by the test setups used to measure impact. Few studies measure impact in vivo (Kohan et al., 2005; Phipps et al., 2006) due to the cost, complexity and ethics of testing in surgery. More common is to study impaction in vitro using cadaveric specimens stripped of soft tissue (Cummins et al., 2011; Fritsche et al., 2008; Jin et al., 2006; Kroeber et al., 2002; Schlegel et al., 2011a,

* Corresponding author.

E-mail addresses: ruben.doyle11@imperial.ac.uk (R. Doyle), o.boughton@imperial.ac.uk (O. Boughton), dan.plant@rheonlabs.com (D. Plant), george.desoutter@desoutter.com (G. Desoutter), j.cobb@imperial.ac.uk (J.P. Cobb), j.jeffers@imperial.ac.uk (J.R.T. Jeffers).

2011b; Stryker, 2012; West and Fryman, 2008) or expanded polyurethane (PU) foams as an analogue for cadaveric bone (Fritsche et al., 2008; Jin et al., 2006; Schmidig et al., 2013). These types of experiment are usually performed with specimens rigidly potted in the test frame of laboratory equipment, or fixed to laboratory benches of unknown stiffness, and ignore the compliance of the body segments and soft tissues that support the acetabulum and femur during the implant impaction strikes.

These rigid test setups may not be an adequate representation of the intraoperative conditions because any movement of the bone during impaction could cushion the impact and attenuate peak forces. For example, the cushioning effect of the trochanteric tissues influence hip fracture risk during a fall, because they attenuate the impact force experienced by the bone (Bouxsein et al., 2007; Laing and Robinovitch, 2010). The relative movement between body segments also influences the peak force – recent studies have found the force transmission during acetabular impact is different for patients of varying body weights (Bullock et al., 2018).

The aim of our study is to create an *in vitro* method for assessing implant impaction in THA that considers the support of the acetabulum and femur by body segments and soft tissues. To achieve this, mechanical compliance of the femur and acetabulum are measured in cadaver specimens and a testing rig is created to replicate these conditions. Such a test setup could provide a more realistic test method for pre-clinical testing of new implant designs or surgical introducer instruments.

2. Methods

2.1. Cadaveric experiment

Following approval from the local Research Ethics Committee four recently deceased intact phenol soft fixed cadavers (mean age 90 [81–94], mean weight 60 kg [50–65], 2 male, 2 female) were prepared for THA by an experienced orthopaedic consultant (JC) using the posterior approach. Bolsters were used to position cadavers mimicking operating theatre conditions. Prior to testing each cadaver was imaged using computed tomography (CT) and each acetabular diameter measured. Press-fit and cemented (Simplex ACR308, Kemdent, Swindon UK) fixtures were used to couple a custom introducer to the acetabulum and pelvis respectively. Both couplings of introducer to bone were chosen to be highly rigid and to minimise relative motion, which could produce an inaccurate estimation of boundary condition values. The custom introducer closely matched the properties of a commercially used straight introducer, with bespoke fittings for the bone fixtures and mounting points for motion tracking markers. To accurately track movement of the whole bone/introducer system the two were rigidly connected.

A custom surgical mallet (700 g) was fitted with a 100 kN impact load cell (200C20, PCB Piezotronics, New York USA) using the manufacturer supplied titanium strike surface. Force data were acquired using a high speed USB Acquisition unit (NI-9234, National Instruments, Newbury UK), sampling at 51.2 kHz. Both surgical mallet and introducer were fitted with passive infrared motion tracking markers. To accurately track movement of the whole bone/introducer system the two were rigidly connected. Displacement data were acquired at 355 Hz, with a Root Mean Square (RMS) error of 90 μm (fusionTrack 500, Atracsys, Switzerland). Fig. 1 shows the experimental setup.

24 impact strikes were applied to the acetabulum and femur. Acetabular impacts were applied at approximately 45° inclination and 20° anteversion with respect to the bolstered pelvis. The femur was internally rotated and held at approximately 30° inclination with the knee held into the surgical assistant's pelvis, representing typical surgery. Impact was directed along the long axis of the

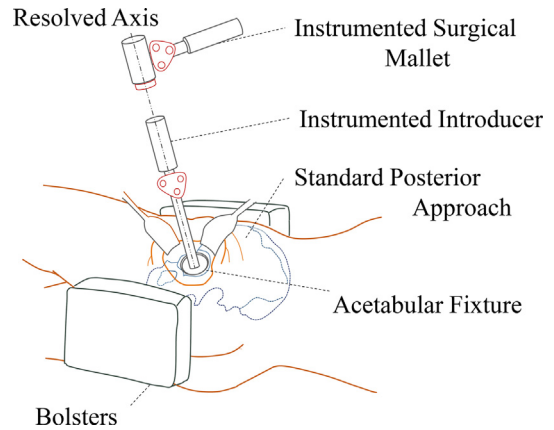


Fig. 1. Experimental setup and axis of resolution for instruments.

femur. Impacts were split into categories, with the surgeon asked to represent 3 levels of impact for each type of implant. A 'Low' level strike would represent a light strike used to broach/seat implants in fragile bone. 'Medium' would simulate strikes used on the most common patient type. 'High' represents the largest impact the surgeon would apply in strong bone.

Each acquired force trace [$P(t)$] was analysed to find peak force for each strike. A numerical integration scheme with respect to time from zero value prior to strike (t_0) to the point at which load transients had fallen away (t_1) was used to determine impulse. Displacement data were transformed to the appropriate axis for each instrument (Fig. 1). Introducer displacement was processed using a low pass, 3rd order Butterworth filter, 8000 Hz cut-off, to remove random tracking error. Mallet displacement was numerically differentiated with respect to time to derive velocity, with the velocity immediately prior to impact (v_i) recorded for each strike. Energy of the strike (E_{strike}) was derived from both impulse and velocity measurements (Eq. (1)) as demonstrated by Maharaj and Jamison (1993))

$$E_{strike} = \frac{v_i}{2} \int_{t_0}^{t_1} P(t) dt \quad (1)$$

2.2. Soft tissue compliance simulation

A numerical mass-spring-damper (MSD) model was required to extract the impaction boundary conditions of the femur and acetabulum from the cadaver test. The measured impulse from the cadaver testing was applied to this model and the MSD variables iterated until the displacement response matched the cadaver test displacement data. The model approximates the rigidly coupled introducer, bone, musculature and upper body (in the case of the acetabulum) or leg (in the case of the femur) as an effective mass, supported by spring and dashpot elements to represent both the stiffness and viscoelasticity of the system. The model approximation is shown in Fig. 2.

The MSD model chosen to approximate the system was an effective mass (m , kg) coupled with parallel spring (k , N/m) and dashpot supports (b , N s/m), known as a Voigt, or Kelvin, model. Preliminary analysis showed a significant level of damping post impact and a poor representation of the system if using mass-spring alone. Voigt models have also previously been used to model tissue response to impulse or step displacement (Fung, 1993).

A Matlab (2015a, Mathworks, MA USA) script using the 'Control Systems Toolbox' was created, producing a displacement trace of a Voigt model in response to a force-time [$P(t)$] input. Impulses were

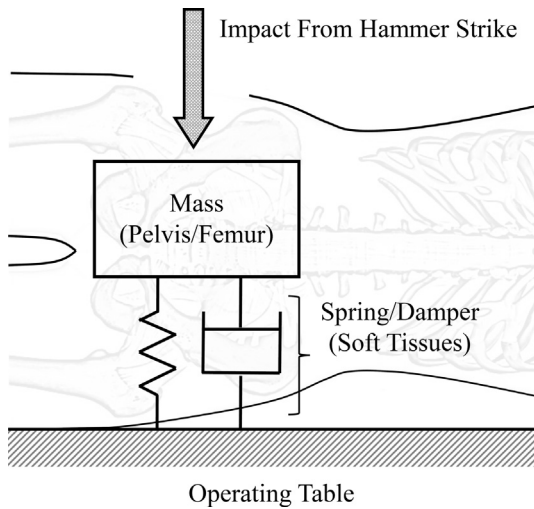


Fig. 2. Approximation of acetabular/femoral soft tissue compliance using a Voigt model.

defined as a half sine wave with a peak equal to that of average peak forces recorded, and area under curve (impulse) equal to those recorded experimentally.

Each Voigt model parameter was varied using numerical iteration. Each simulated displacement trace was subtracted from the corresponding experimental trace and the resulting array used to calculate RMS error. The lowest average error simulated strike for each Voigt setup was recorded. Mass, stiffness and damping increments of 0.001 kg, 1 N/m and 0.01 N s/m were evaluated respectively. These data were then used to define the boundary conditions of the in vitro impact rig.

A sensitivity analysis investigated the influence of the MSD parameters on the output displacement trace. A One-At-a-Time (OAT) approach was used. With the other two parameters held at their final calculated values, each of Mass, Stiffness and Damping were changed to 0.5 and 1.5 times their calculated value, and the peak displacement and rise time recalculated. The subsequent gradient was used to define sensitivity.

2.3. In vitro impact testing rig

An impact rig was built to simulate the impact boundary conditions of the cadaver test. The base of this rig, upon which the impact occurs, was a translatable platen supported by a parallel spring and dashpot to replicate the Voigt model determined in Section 2.2. The mass of the platen, spring stiffness and dashpot coefficient were defined by the output of the Voigt model described in Section 2.2.

A drop weight, fitted with the same load cell in Section 2.2 provided impact with adjustable velocity and mass (Fig. 3). Due to errors in approximating impact velocity from a drop height, a light gate was used to determine the velocity of the drop weight immediately before impact. A 50 mm stroke LVDT (S025.0, Solartron Metrology, Bognor Regis UK) was used to measure the displacement of the platen. A surgical introducer of the same mass and impact surface as the custom introducer in Section 2.1 was rigidly coupled to a 30PCF Sawbone block (Sawbone Europe AB, Malmö Sweden).

The mass of the drop weight was set to match that of the custom mallet used in Section 2.1 (700 g). Velocity was set to values obtained during cadaveric testing (Section 3.1.2). Six strikes were carried out for each of the following six categories, to match the cadaver data: Low, Medium and High strikes for both acetabulum

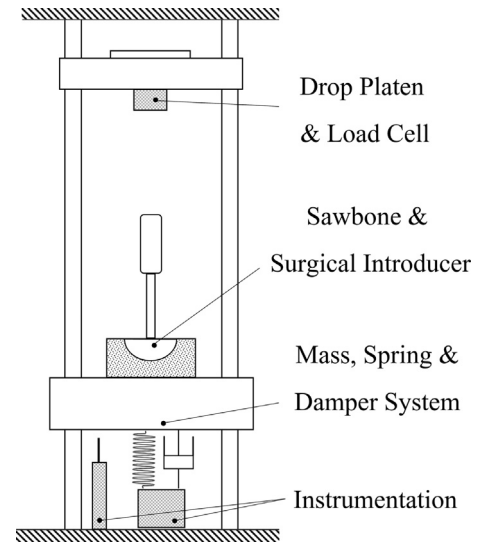


Fig. 3. In vitro drop rig setup.

and femur. For each of the strikes, impact force, impulse, velocity and energy were measured. From the recorded impact platen displacement both peak displacement and rise time were recorded (defined in Fig. 4). These metrics were chosen as they have previously been identified as appropriate to characterise impact (Derler et al., 2005; Etheridge et al., 2005; Laing and Robinovitch, 2010).

2.4. Statistical data analysis

In order to determine whether the data from the acetabulum and femur should be averaged or analysed separately before being used as inputs to the Matlab Voigt model, statistical analyses were performed. The influence of anatomical site at each strike level upon peak force and impulse was analysed. First, peak force and impulse data were tested for normality with Shapiro-Wilk test in SPSS (v24, IBM, NY). Data were then analysed with two-way repeated measures analyses of variance with first the measured peak force, and then with impulses data as the dependent variable. For each dependent variable a RMANOVA was performed with independent variables of anatomy (femur/acetabulum) and intended strike force (low, med, high).

Additional analyses were carried out to determine whether it was appropriate to average or keep compliance values separate for each strike level. Two-way RMANOVAs were used, with Mass, Spring Stiffness and Damping Coefficient as the dependant variables. Anatomy and strike level were set as the independent variables. Main effects were considered if no two-way dependency was found.

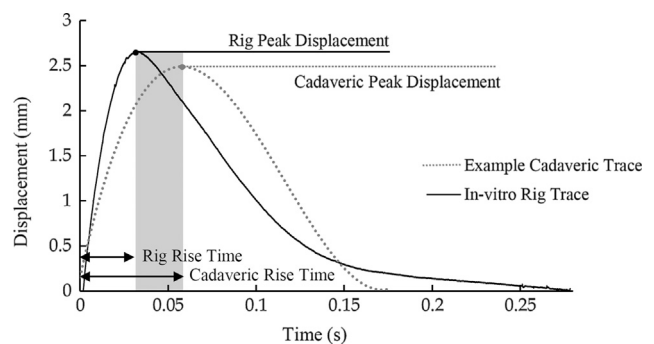


Fig. 4. Example displacement traces from cadaveric and in-vitro rig testing.

The significance level was set to $p < 0.05$. Post-hoc paired t -tests with Bonferroni correction were applied when differences across tests were found. Adjusted p -values, multiplied by the appropriate Bonferroni correction factor in SPSS, have been reported rather than reducing the significance level. Post-hoc power analyses were conducted in G*Power (v3.1.9.2, Universität Kiel, Germany) for strike force and mass, spring and dashpot values when comparing anatomy. A minimum power value of 0.63 was achieved, with an average of 0.76.

3. Results

3.1. Cadaveric experiment

3.1.1. Force and impulse

The effect of intended strike level (low, medium, high) was dependent on the anatomical site (femur/acetabulum) ($p < 0.0005$). For all strikes, lower forces were measured for the femur than the acetabulum, however the difference increased with increasing strike force: At a low strike level a 23% difference in mean was observed ($1930 \text{ N} \pm 502$, $p = 0.031$), 15% at medium strike level ($2570 \text{ N} \pm 490$, $p < 0.0005$), and 29% at high strike level ($8630 \text{ N} \pm 414$, $p < 0.0005$). The same was observed for impulse data, with the effect of anatomical site dependent on the intended strike level, and the femur always lower than the acetabulum ($p < 0.0005$, Table 1). Due to the differences, femoral and acetabular data were separated in subsequent analyses.

3.1.2. Velocity and energy

Table 2 presents the mean measured velocity for each intended strike level for both femoral and acetabular anatomical sites, and the resultant energy of the impact. Velocity values were used as input velocities for the in vitro rig described in Section 3.3.

3.2. Soft tissue compliance simulation

Data for one hip could not be collected due to the cadaver already having had a unilateral THA prior to death. Traces were

split into individual strikes and time, and initial displacement was zeroed for each. A total of 174 strikes were analysed, with an average of 24 usable data sets for each hip. Each was analysed using the Matlab script described in Section 2.2.

A typical displacement trace of the acetabulum or femur was characterised by an initial acceleration as momentum transferred from the surgical mallet, followed by a damped return to the initial zero position.

The model indicated the main effect of anatomical site (i.e. acetabulum or femur) showed a statistical difference in output for both mass ($p = 0.02$) and damping coefficient ($p = 0.009$), but not spring stiffness ($p = 1.0$). As both mass and damping showed differences at each anatomical site, setups for femoral and acetabular testing are separate.

The model spring stiffness showed no difference between low and medium, medium and high and low and high strike levels ($p = 1.00$, $p = 0.3$, $p = 0.7$). The model did detect differences in effective mass between low and high ($p < 0.0005$) and medium and high ($p = 0.03$) but not low and medium strike levels ($p = 1.00$). The main effect for intended strike level upon damping coefficient was only significant for low and high strikes ($p = 0.03$). Due to differences only being found between certain strike levels it was decided that mass, spring stiffness and damping coefficient would be averaged over the three strike levels for each anatomical site (see 'average' strike level in Table 3). This decision was compounded by the desire for a testing setup that was as simple as possible, negating the need for constant compliance adjustment for different strike levels.

A summary of Effective Mass, Spring Stiffness and Damping Coefficient outputs can be found in Table 3.

3.3. Results: in-vitro rig

For the acetabulum no differences between the test rig and cadaver traces were detected for peak displacement and rise time (Fig. 5). The peak displacement increased from 2.5 mm for the surgeon's low strike force to 6 mm for the high strike force, but the rise time remained constant, at around 30 ms, for all three applied strike forces.

Table 1
Cadaveric peak force and impulse data with significance values.

Strike level	Force (kN)							p
	Acetabular			Femoral				
	Mean	SD	N	Mean	SD	N		
Low	8.24	1.15	18	6.31	0.86	25	0.03	
Medium	17.10	1.60	15	14.53	1.57	24	<0.005	
High	30.26	8.08	12	21.63	1.29	21	<0.005	
	Impulse (Ns)							
	Acetabular			Femoral				
	Mean	SD	N	Mean	SD	N	p	
Low	1.775	0.217	19	1.176	0.211	24	<0.005	
Medium	2.892	0.590	14	2.335	0.399	24	<0.005	
High	4.757	1.260	12	4.033	0.896	22	<0.005	

Table 2
Cadaveric mallet velocity and calculated energy.

Strike level	Peak mallet velocity (m/s)						Calculated energy (J)			
	Acetabular			Femoral			Acetabular		Femoral	
	Mean	SD	N	Mean	SD	N	Mean	SD	Mean	SD
Low	3.86	0.46	59	2.14	0.30	44	3.42	0.58	1.26	0.29
Med	6.10	0.79	41	4.15	0.62	13	8.81	2.13	4.84	1.10
High	7.45	0.52	54	5.34	1.18	19	17.71	4.85	10.78	3.38

Table 3
Mass, spring stiffness and dashpot coefficients matched to experimental traces.

Strike level	Acetabular								
	Mass (<i>m</i> , kg)			Spring stiffness (<i>k</i> , kN/m)			Dashpot coefficient (<i>b</i> , N s/m)		
	Mean	SD	N	Mean	SD	N	Mean	SD	N
Low	18.4	5.4	41	7.4	2.5	41	547	88	42
Med	17.0	4.6	29	8.4	2.8	28	585	116	28
High	23.7	5.1	30	8.3	3.6	29	664	143	30
Mean	19.7	5.1	100	8.0	3.0	98	595	114	100
	Femoral								
Low	11.7	3.6	34	3.1	1.3	34	289	71	34
Med	10.6	1.0	21	3.5	0.6	21	290	28	21
High	15.9	2.6	19	5.6	1.5	19	389	61	19
Mean	12.7	2.8	74	4.1	1.2	74	322	59	74

For the femur, no differences were detected between the test rig and cadaver traces for peak displacement. The peak displacement increased from 3 mm for the surgeon's low strike force to 5.6 mm for the high strike force. The test rig also matched the rise time for the surgeon's low and high impact strikes, but a 0.6 ms difference was detected for the surgeon's medium strike force. As with the acetabular data, the rise time did not vary with the surgeon's strike level.

The sensitivity study indicated the peak displacement was more sensitive to MSD parameters at higher strike levels for the femur and acetabulum, and the femoral peak displacement was more sensitive to MSD parameters than the acetabular (Table 4). The rise time sensitivity was not affected by strike level, but was more sensitive to MSD parameters for the femur than acetabulum. The only detected difference between the cadaver and test rig displacement traces was the rise time for the medium strike level acetabulum. The sensitivity analysis indicated an error of 2.2 kg mass, or 0.37 kN/m spring constant, or 149 N s/m damping could cause this difference.

4. Discussion

The most important finding of this study is that the mechanical compliance of the acetabulum and femur can be measured in vivo

and replicated with a physical representation of a Voigt model. When a hammer impact is applied to the acetabulum or femur, the bone is displaced by between 2.5 and 6 mm over a duration of around 30 ms (between 80 and 200 $\mu\text{m}/\text{ms}$). This displacement is caused by the bone being supported by the non-rigid soft tissues and body segments of the musculoskeletal system. This boundary condition may influence the force experienced by the acetabulum during implant seating (Bullock et al., 2018; Maharaj and Jamison, 1993). Our paper presents a method to replicate these boundary conditions using a spring and dashpot system.

The impact magnitudes measured and replicated in this study fall within the range of existing literature (Maharaj and Jamison, 1993, Phipps et al., 2006, West and Fryman, 2008, Kohan et al., 2005). Maharaj and Jamison (1993) found similar femoral impaction energy (4.5 J) but a peak force that was lower (6.2 kN) than measured here. The discrepancy in peak force could be explained by the polyacetal (Delrin™) tipped mallet used by Maharaj, attenuating peak force but transferring similar energy as the titanium tipped mallet used in this study. Our mallet velocities were also found to be within 20% of Maharaj's values. Peak force values measured intraoperatively for acetabular cup insertion and femoral rasping by West and Fryman (2008), Phipps et al. (2006) and Kohan et al. (2005) also fall within the values measured during this study. Additionally, variation of measurements are also of similar magnitude to the difference between 'low' and 'high' strike force

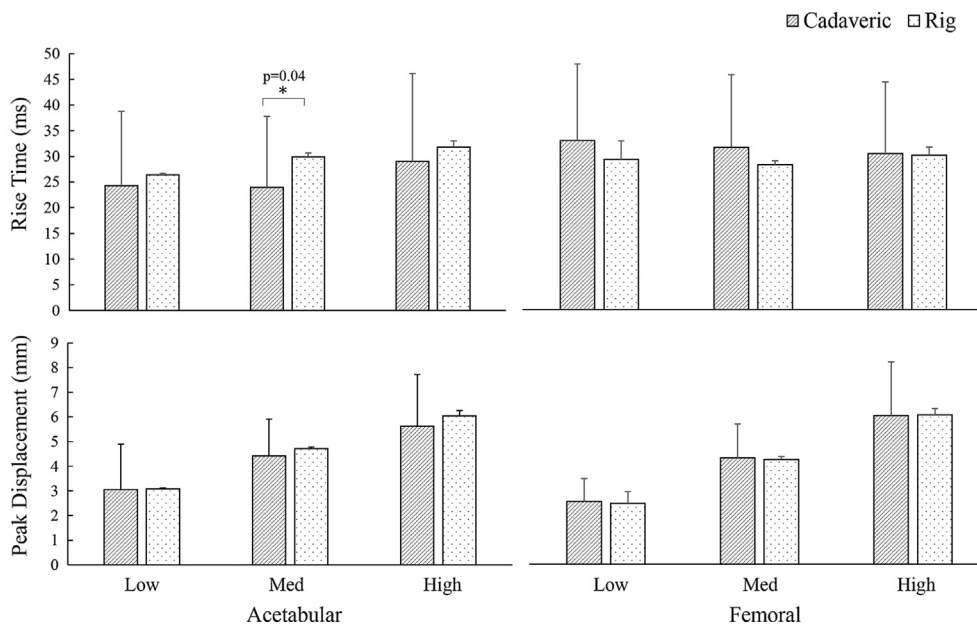


Fig. 5. Comparison between peak displacement and rise time for cadaveric and rig measurements.

Table 4
Displacement parameters statistics and sensitivity study.

Strike level		Peak displacement			Simulation sensitivity			Possible error due to difference		
		Cadaveric vs Rig		<i>p</i>	Mass (<i>m</i> , mm/kg)	Spring stiffness (<i>k</i> , mm/[kN/m])	Damping (<i>b</i> , mm/[N s/m])	Mass (kg)	Spring (kN/m)	Damping (N s/m)
		Absolute (mm)	%							
Acetabular	Low	0.03	0.85	0.93	0.035	0.086	0.0030	0.74	0.30	8.71
	Med	0.30	6.89	0.30	0.056	0.139	0.0048	5.39	2.19	63.4
	High	0.43	7.60	0.39	0.091	0.222	0.0077	4.71	1.91	55.4
Femoral	Low	0.07	2.78	0.97	0.068	0.213	0.0061	1.05	0.34	11.8
	Med	0.07	1.65	0.79	0.130	0.400	0.0116	0.55	0.18	6.18
	High	0.03	0.51	0.95	0.233	0.714	0.0208	0.13	0.04	1.50
		Rise Time								
		Absolute (ms)	%	<i>p</i>	Mass (ms/kg)	Spring (ms/[kN/m])	Damping ([ms/[N s/m])	Mass (kg)	Spring (kN/m)	Damping (N s/m)
Acetabular	Low	2.02	8.30	0.39	2.7	15.9	0.040	0.75	0.13	51.0
	Med	5.91	24.7	0.04*	2.7	15.9	0.040	2.20	0.37	149
	High	2.77	9.53	0.43	2.7	15.9	0.040	1.03	0.17	69.7
Femoral	Low	3.59	11.2	0.47	4.8	37.0	0.079	0.76	0.10	45.4
	Med	3.37	10.9	0.22	4.8	37.0	0.079	0.71	0.09	42.6
	High	0.30	1.02	0.92	4.8	37.0	0.079	0.06	0.01	3.82

measured for our consultant surgeon. Importantly, in these three studies, at these peak forces measured, few fractures of the bone were encountered. These three studies measured forces in cadavers or live patients, and thus had appropriate compliance boundary conditions to the acetabulum/femur. In contrast, a study by Cummins et al. (2011) report bone fracture at loads of 1.6 kN. This study used a rigid potting of the bone in a solid fixture with no compliant boundary condition. Thus, more of the energy in the impact may have been transmitted into the bone and not the surrounding tissue, and this could explain such a large reduction in peak force to fracture in these two studies.

While no direct comparison of Voigt model parameters for the hip can be made to other studies for intraoperative impact there is significant work determining model values for the hip during falls. Robinovitch et al. have found both effective mass of the hip and dashpot coefficients in a similar range and sensitivity to the results of this study (Robinovitch et al., 1997a, 1997b).

A limitation of the Voigt model is that it does not predict an instantaneous spike in force during impact. However, previous studies have found adaptation of the Voigt to a Standard Linear Solid arrangement (with series spring and dashpot in place of the dashpot of a Voigt) offers only a small improvement in response prediction (Robinovitch et al., 1997a, 1997b). A further improvement to this study would be to include a measurement of force within the hip cadaver system. Force data could provide further validation of the impact mechanics of the system. However such measurement would require a highly complex setup. An advantage of the methodology used in this study is that the methods described could be used to gather data in the operating room; an even more representative scenario.

A further limitation of this study is the use cadavers of similar weight and age. Patients of these BMIs and ages may not be selected for cementless arthroplasty. If possible the same methodology should be used with higher body mass index (BMI) cadavers of a lower age, where different Voigt model parameters might be expected, such as slightly higher effective mass, as found by Levine et al. (2013). With further research it would be useful to characterise the effects of BMI, soft tissue thickness, sex, age and other factors. In addition, it is known that cadaveric tissue may not behave the same as living tissue. This was mitigated as much as possible by using phenol embalmed specimens rather than formaldehyde or formalin fixed, both known to alter tissue proper-

ties (Brenner, 2014). Furthermore, only one surgeon performed the cadaver work, whereas a larger number of surgeons would be useful to determine the average magnitude of impact in THA. However, the surgeon's three different strike values provide some information on the strike range that may exist, and these data agreed well with prior work.

For very short duration events such as hard on hard contact between a hammer and introducer, or modular femoral head seating, replicating the compliance of the body segments may not be necessary. This is because the impact event is very short and the seating event is over before the implant/body segment has had time to accelerate (Krull et al., 2017). However for a softer impact event, such as the introduction of an acetabular cup or femoral stem into a bony cavity, impact events are longer. Several studies have shown event durations of a similar magnitude to the rise time found in this study (Hothi et al., 2011; Mathieu et al., 2013; Michel et al., 2015; Tang et al., 2016). Therefore compliance is a much more relevant consideration as the body segments are accelerated by the implant/introducer in a similar timescale as impact duration. This may have an effect on experimental results.

Hip compliance has been recognised as a possible factor in implant seating and several groups have attempted to include this boundary condition in their testing (Nambu et al., 2018; Nassutt et al., 2006; Scholl et al., 2016) but have not been able to validate the compliance properties of their supports with *in-vivo* data. This paper provides a method to recreate the *in-vivo* compliance of the femur and acetabulum in a laboratory drop rig or computational model. Including this boundary condition in preclinical testing may provide an improved representation of the clinical conditions necessary to investigate implant seating.

Conflict of interest statement

The institution of one or more of the authors (JJ, RD) has received funding from Desoutter Medical and the Engineering and Physical Sciences Research Council.

Ethical review committee statement

Appropriate ethical approval was obtained for the use of human tissues during this study. The corresponding letter of approval (R15022-1A) is attached.

Location of work statement

Cadaveric testing was carried out in the Department of Surgery & Cancer, Charing Cross Campus, Imperial College London, London, UK, while all analysis and in vitro work was carried out in the Department of Mechanical Engineering, South Kensington, Campus, Imperial College London, London, UK.

Acknowledgements

We thank Kartik Logishetty, Sam Vargas and Rachael Waddington for their invaluable assistance during cadaveric testing. We would also like to thank Aply Rosevere for his expertise in high speed acquisition when building our in vitro drop tower and Lesley Honeyfield for her assistance in CT scanning the cadavers. Funding for this study was obtained by the institution of one or more of the authors (RD, JJ) from Desoutter Medical and the UK Engineering and Physical Sciences Research Council (grant no: EP/K027549/1).

References

- American Joint Replacement Registry, 2016. Third AJRR Annual Report on Hip and Knee Arthroplasty Data 2016.
- Benazzo, F., Formagnana, M., Bargagliotti, M., Perticarini, L., 2015. Periprosthetic acetabular fractures. *Int. Orthop.* 39, 1959–1963. <https://doi.org/10.1007/s00264-015-2971-8>.
- Bouxein, M.L., Szulc, P., Munoz, F., Thrall, E., Sornay-Rendu, E., Delmas, P.D., 2007. Contribution of trochanteric soft tissues to fall force estimates, the factor of risk, and prediction of hip fracture risk. *J. Bone Miner. Res.* 22, 825–831. <https://doi.org/10.1359/jbmr.070309>.
- Brenner, E., 2014. Human body preservation – old and new techniques. *J. Anat.* 224, 316–344. <https://doi.org/10.1111/joa.12160>.
- Bullock, M.W., De Gregorio, M., Danelson, K.A., Willey, J.S., Seem, M.E., Plate, J.F., Lang, J.E., Shields, J.S., 2018. Quantifying the force transmission through the pelvic joints during total hip arthroplasty: a pilot cadaveric study. *Clin. Biomech.* 58, 69–73. <https://doi.org/10.1016/j.clinbiomech.2018.07.013>.
- Cummins, F., Reilly, P.O., Flannery, O., Kelly, D., Kenny, P., 2011. Defining the impaction frequency and threshold force required for femoral impaction grafting in revision hip arthroplasty. A human cadaveric mechanical study. *Acta Orthop.* 82, 433–437. <https://doi.org/10.3109/17453674.2011.594228>.
- Daniel, J., Ziaee, H., Kamali, A., Pradhan, C., McMinn, D., 2012. What are the risks accompanying the reduced wear benefit of low-clearance hip resurfacing? *Clin. Orthop. Relat. Res.* 470, 2800–2809. <https://doi.org/10.1007/s11999-012-2476-3>.
- Derler, S., Spierings, A.B., Schmitt, K.U., 2005. Anatomical hip model for the mechanical testing of hip protectors. *Med. Eng. Phys.* 27, 475–485. <https://doi.org/10.1016/j.medengphy.2005.02.001>.
- Etheridge, B.S., Beason, D.P., Lopez, R.R., Alonso, J.E., McGwin, G., Eberhardt, A.W., 2005. Effects of trochanteric soft tissues and bone density on fracture of the female pelvis in experimental side impacts. *Ann. Biomed. Eng.* 33, 248–254. <https://doi.org/10.1007/s10439-005-8984-5>.
- Flannery, O.M., Britton, J.R., O'Reilly, P., Mahony, N., Prendergast, P.J., Kenny, P.J., 2010. The threshold force required for femoral impaction grafting in revision hip surgery – a preliminary study in sow femurs. *Acta Orthop.* 81, 303–307. <https://doi.org/10.3109/17453674.2010.480936>.
- Fritsche, A., Bialek, K., Mittelmeier, W., Simnacher, M., Fethke, K., Wree, A., Bader, R., 2008. Experimental investigations of the insertion and deformation behavior of press-fit and threaded acetabular cups for total hip replacement. *J. Orthop. Sci.* 13, 240–247. <https://doi.org/10.1007/s00776-008-1212-z>.
- Graves, S., De Steiger, R., Lewis, P., Williams, S., Bergman, N., Cunningham, J., 2014. Australian orthopaedic association national joint replacement registry. *Aust. Orthop. Assoc. Natl. Jt. Regist.*
- Hartford, J.M., Knowles, S.B., 2018. Risk factors for perioperative femoral fractures: cementless femoral implants and the direct anterior approach using a fracture table. *J. Arthroplasty* 31, 2016. <https://doi.org/10.1016/j.arth.2016.02.045>.
- Hothi, H.S., Busfield, J.J.C., Shelton, J.C., 2011. Explicit finite element modelling of the impaction of metal press-fit acetabular components. *Proc. Inst. Mech. Eng. Part H J. Eng. Med.* 225, 303–314. <https://doi.org/10.1243/09544119JEM864>.
- Jin, Z.M., Meakins, S., Morlock, M.M., Parsons, P., Hardaker, C., Flett, M., Isaac, G., 2006. Deformation of press-fitted metallic resurfacing cups. Part 1: experimental simulation. *Proc. Inst. Mech. Eng. H* 220, 299–309. <https://doi.org/10.1243/095441105X69150>.
- Kohan, L., Appleyard, R., Hogg, M., Donohoo, S., Gillies, R., 2005. Impaction loads during the insertion of hip resurfacing components. 53rd Annu. Meet. Orthop. Res. Soc. 36, Poster No 1701.
- Kroeber, M., Ries, M.D., Suzuki, Y., Renowitzky, G., Ashford, F., Lotz, J., 2002. Impact biomechanics and pelvic deformation during insertion of press-fit acetabular cups. *J. Arthroplasty* 17, 349–354. <https://doi.org/10.1054/arth.2002.30412>.
- Krull, A., Bishop, N.E., Steffen, N.M., Lampe, F., Püschel, K., Morlock, M.M., 2017. Influence of the compliance of a patient's body on the head taper fixation strength of modular hip implants. *Clin. Biomech.* 46, 1–5. <https://doi.org/10.1016/j.clinbiomech.2017.04.009>.
- Laing, A.C., Robinovitch, S.N., 2010. Characterizing the effective stiffness of the pelvis during sideways falls on the hip. *J. Biomech.* 43, 1898–1904. <https://doi.org/10.1016/j.jbiomech.2010.03.025>.
- Langdown, A.J., Pickard, R.J., Hobbs, C.M., Clarke, H.J., Dalton, D.J.N., Grover, M.L., 2007. Incomplete seating of the liner with the Trident acetabular system: a cause for concern? *J. Bone Jt. Surg. Br.* 89–B, 291–295. <https://doi.org/10.1302/0301-620X.89B3.18473>.
- Levine, I.C., Bhan, S., Laing, A.C., 2013. The effects of body mass index and sex on impact force and effective pelvic stiffness during simulated lateral falls. *Clin. Biomech.* 28, 1026–1033. <https://doi.org/10.1016/j.clinbiomech.2013.10.002>.
- Lindberg-larsen, M., Jørgensen, C.C., Solgaard, S., Anne, G., 2017. Increased risk of intraoperative and early postoperative periprosthetic femoral fracture with uncemented stems Increased risk of intraoperative and early postoperative periprosthetic femoral fracture with uncemented stems 7, 169 total hip arthroplasty. *Acta Orthop.* 3674, 8–13. <https://doi.org/10.1080/17453674.2017.1302908>.
- Maharaj, G., Jamison, R., 1993. Intraoperative impact: characterization and laboratory simulation on composite hip prostheses. *Compos. Mater. Implant Appl. Hum. Body Charact. Testing. ASTM STP 1178*.
- Masri, B.A., Meek, R.M.D., Duncan, C.P., 2004. Periprosthetic fractures evaluation and treatment. *Clin. Orthop. Relat. Res.* 80–95. <https://doi.org/10.1097/01.blo.0000122241.70546.eb>.
- Mathieu, V., Michel, A., Flouzat Lachaniette, C.H., Poignard, A., Hernigou, P., Allain, J., Haïat, G., 2013. Variation of the impact duration during the in vitro insertion of acetabular cup implants. *Med. Eng. Phys.* 35, 1558–1563. <https://doi.org/10.1016/j.medengphy.2013.04.005>.
- Michel, A., Bosc, R., Vayron, R., Haïat, G., 2015. In vitro evaluation of the acetabular cup primary stability by impact analysis. *J. Biomech. Eng.* 137, 31011. <https://doi.org/10.1115/1.4029505>.
- Nambu, S., Ewing, M., Timmerman, L., Roark, M., Fitch, D., 2018. Effect of assembly impaction and cyclic loading forces on the micromotion. *The Modular Neck-Stem Interface*, in: Orthopaedic Proceedings. Bone & Joint Publishing, London.
- Nassutt, R., Mollenhauer, I., Klingbeil, K., Hennig, O., Grundei, H., 2006. Die Bedeutung der Setzkraft für die Sicherheit einer Konuskopplung von Hüftstiel und keramischem Prothesenkopf/Relevance of the insertion force for the taper lock reliability of a hip stem and a ceramic femoral head. *Biomed. Tech. Eng.* 51, 103–109. <https://doi.org/10.1515/BMT.2006.018>.
- NJR Editorial Board, 2014. National Joint Registry – England, Wales & Northern Ireland.
- Pedersen, A.B., Fenstad, A.M., 2016. Nordic Arthroplasty Register Association Report 2016.
- Phipps, K., Saksena, J., Muirhead-Allwood, S., Miles, A., Goodship, A., Blunn, G., 2006. Evaluation of femoral impaction grafting forces. *Bone Joint J.* 373
- Rehmer, A., Bishop, N.E., Morlock, M.M., 2012. Influence of assembly procedure and material combination on the strength of the taper connection at the head-neck junction of modular hip endoprotheses. *Clin. Biomech.* 27, 77–83. <https://doi.org/10.1016/j.clinbiomech.2011.08.002>.
- Robinovitch, S.N., Hayes, W.C., McMahon, T.A., 1997a. Distribution of contact force during impact to the hip. *Ann. Biomed. Eng.* 25, 499–508. <https://doi.org/10.1007/BF02684190>.
- Robinovitch, S.N., Hayes, W.C., McMahon, T.A., 1997b. Predicting the impact response of a nonlinear single-degree-of-freedom shock-absorbing system from the measured step response. *J. Biomech. Eng.* 119, 221–227. <https://doi.org/10.1115/1.2796083>.
- Schlegel, U.J., Knifka, J., Röllinghoff, M., Koebke, J., Eysel, P., Morlock, M.M., 2011a. Effects of impaction on cement mantle and trabecular bone in hip resurfacing. *Arch. Orthop. Trauma Surg.* 131, 459–464. <https://doi.org/10.1007/s00402-010-1147-7>.
- Schlegel, U.J., Rothstock, S., Siewe, J., Schiwy-Bochat, K.H., Eysel, P., Morlock, M.M., 2011b. Does Impaction Matter in Hip Resurfacing? A cadaveric study. *J. Arthroplasty* 26, 296–302. <https://doi.org/10.1016/j.arth.2010.01.108>.
- Schmidig, G., Scholl, L., Thakore, M., Faizain, A., 2013. Evaluation of Variability in Head Impaction Forces Among Multiple Orthopaedic Surgeons.
- Scholl, L., Schmidig, G., Faizan, A., TenHuisen, K., Nevelos, J., 2016. Evaluation of surgical impaction technique and how it affects locking strength of the head-stem taper junction. *Proc. Inst. Mech. Eng. Part H J. Eng. Med.* 230, 661–667. <https://doi.org/10.1177/0954411916644477>.
- Sharkey, P.F., Hozack, W.J., Callaghan, J.J., Kim, Y.S., Berry, D.J., Hanssen, A.D., LeWallen, D.G., 1999. Acetabular fracture associated with cementless acetabular component insertion: a report of 13 cases. *J. Arthroplasty* 14, 426–431. [https://doi.org/10.1016/S0883-5403\(99\)90097-9](https://doi.org/10.1016/S0883-5403(99)90097-9).
- Squire, M., Griffin, W.L., Mason, J.B., Peindl, R.D., Odum, S., 2006. Acetabular component deformation with press-fit fixation. *J. Arthroplasty* 21, 72–77. <https://doi.org/10.1016/j.arth.2006.04.016>.
- Stryker, 2012. A novel test method to characterize intraoperative impacts during femoral broaching and stem insertion. In: ORS, p. 2012.
- Tang, L., Tennant, J.K., Forster, A., Reddy, M., 2016. Acetabular cup seating impact sensing for press-fit acetabular cup fixation. *MESA 2016 – 12th IEEE/ASME Int. Conf. Mechatron. Embed. Syst. Appl. – Conf. Proc.*

- Thien, T.M., Chatziagorou, G., Garellick, G., Furnes, O., Havelin, L.L., Mäkelä, K., Overgaard, S., Pedersen, A., Eskelinen, A., Pulkkinen, P., Kärrholm, J., 2014. Periprosthetic femoral fracture within two years after total hip replacement: analysis of 437,629 operations in the nordic arthroplasty register association database. *J Bone Jt. Surg Am.* 96, e167. <https://doi.org/10.2106/JBJS.M.00643>.
- Thillemann, T.M., Pedersen, A.B., Johnsen, S.P., Søballe, K., 2008. Inferior outcome after intraoperative femoral fracture in total hip arthroplasty. *Acta Orthop.* 79, 327–334. <https://doi.org/10.1080/17453670710015210>.
- West, C., Fryman, J.C., 2008. Cadaveric measurement of impact force on total hip arthroplasty surgical instrumentation. In: *Am. Soc. Biomech. Annu. Conf. Ann Arbor, Michigan, USA*, p. 173.
- Fung, Y.C., 1993. *Mechanical Properties of Living Tissues*. Springer-Verlag, New York.